Supplemental Materials

Molecular Biology of the Cell

Gon et al.

Supplemental Figure S1. Single-cell polarization of cultured epithelial cells. (A) EpH4 and MDCK cells were plated on Matrigel for 6 h and stained for pEzrin (green) and F-actin (red). (B) The numbers of polarized cells in indicated cell lines among at least 100 cells were counted, and the percentages of polarized cells were calculated. The ratios of the percentages of polarized cells were compared with the controls. (C) (Left panels) IEC6 cells were plated on Matrigel for 2 h and stained for PKCζ (green) and F-actin (red). (Right panels) Live-cell imaging of IEC6 cells stably expressing LifeAct-mCherry and GFP-PLCδ1-PH (PtdIns (4, 5) P2-binding PH domain of PLC). Typical polarized and non-polarized cells were shown in the upper and lower panels, respectively. (D) IEC6 cells stably expressing GFP-actin were plated on Matrigel in a glass-bottomed dish, and time-lapse images were taken by LSM at the indicated times. (E) (Left panel) Expression of *Mst4* mRNA 48 h after siRNA transfection was determined by quantitative real-time PCR (qPCR) and normalized to GAPDH expression. (Right panel) Mst4-depleted IEC6 cells were plated on Matrigel. The results are shown as means ± SD from three independent experiments. (F) IEC6 cells were cultured in suspension (upper panels) or on type I collagen (lower panels) and stained for pEzrin (green) and F-actin (red). (G) IEC6 cells were plated on Matrigel-coated dishes two dimensionally for 8 h and the cells were stained for F-actin. Scale bars in (A), (C), (D), and (F), 5 μm; in (G), 10 μm.

Supplemental Figure S2. Expression level of genes examined in this study. (A) IEC6 cells were transfected with siRNAs for LRP6 or β-catenin and the lysates were probed with anti-LRP6 or anti-β-catenin antibody. β-Tubulin and clathrin were used as loading controls. (B) mRNA expression of Wnt ligands in IEC6 cells were determined by qPCR and normalized to GAPDH. The results are shown as relative expression levels for Wnt2b. (C) The lysates of EpH4 and MDCK cells were probed with anti-Wnt5a antibody. Clathrin was used as a loading control. (D) Parental IEC6 cells or IEC6 cells stably expressing GFP, Wnt5a, or GFP-Dvl2 were transfected with Wnt5a siRNAs and the lysates were probed with anti-Wnt5a antibody. siWnt5a-1, against the open reading frame; siWnt5a-2, against the 3'-untranslated region, respectively. HSP90 was used as a loading control. (E) Parental IEC6 cells or IEC6 cells stably expressing GFP or GFP-Dvl2 were transfected with the indicated siRNAs, and the expression level of *Wnt4*, *Wnt11*, or *Ror1* mRNAs was determined by qPCR and normalized to GAPDH expression. (F) Parental IEC6 cells or IEC6 cells stably expressing GFP, GFP-Dvl2, or Myc-Tiam1 were transfected with the indicated siRNAs, and the lysates were probed with anti-Dvl, anti-Myc and anti-clathrin antibodies. SiDvl2-1, against the open reading frame; siDvl2-2, against the 3'-untranslated region. SiDvls-1, a mixture of siDvl1, siDvl2-1, and siDvl3; siDvls-2, a mixture of siDvl1, siDvl2-2, and siDvl3. (G) IEC6 cells were transfected with Rac1 siRNAs and the lysates were probed with anti-Rac1 and anti-β-tubulin antibodies. (H) Parental IEC6 cells or IEC6 cells stably expressing GFP, GFP-Dvl2, or Myc-Tiam1 were transfected with the indicated siRNAs, and the lysates were probed with anti-Tiam1, anti-Myc, anti-GFP, anti-HSP90 and anti-β-tubulin antibodies. SiTiam1-1, against the 3'-untranslated region; siTiam1-2 and siTiam1-3, against the open reading frame. (I) Parental IEC6 cells or IEC6 cells stably expressing GFP or p190RhoGAP-A were transfected with the indicated siRNAs and the lysates were probed with anti-p190RhoGAP-A and anti-clathrin antibodies. Sip190RhoGAP-A-1, against the open reading frame;

sip190RhoGAP-A-2, against the 3'-untranslated region. (J) IEC6 cells stably expressing GFP-Dvl2 (1-509) were transfected with the siDvls-2 siRNA, and the lysates were probed with anti-GFP, anti-Dvl2 and anti-clathrin antibodies.

Supplemental Figure S3. The localization of PKCζ and ZO-1 in Wnt5a- or Dvls-depleted IEC6 cells. Wnt5a- or Dvls-depleted IEC6 cells were plated on Matrigel for 2 h and stained for PKCζ or ZO-1 (green) and F-actin (red). Scale bar, 5 μm.

Supplemental Figure S4. Wnt5a signaling is required for the polarized distribution of Rac1 and RhoA activities. (A) IEC6 cells were plated on Matrigel for the indicated time periods and then lysed and incubated with GST-CRIB or GST-RBD immobilized on glutathione-Sepharose. The total lysates (total Rac1 or RhoA, lower panels) and precipitates (active Rac1 or RhoA, upper panels) were probed with anti-Rac1 (left panels) or RhoA antibody (right panels). Susp., suspension. (B) The signals of active Rac1 or RhoA in (A) were quantified using ImageJ and expressed as arbitrary units compared with the signal intensity at time 0 in control cells (Rac1; ■, RhoA; ◆). (C) Wnt5a- (left panels) or Dvls- (right panels) depleted Raichu-Rac1 or Raichu-RhoA expressing IEC6 cells were plated on Matrigel in a glass-bottomed dish for 2 h. Representative FRET/TFP ratio images in Matrigel-contacting area (bottom) and -non-contacting area (top) are shown in the intensity-modulated display mode. The upper and lower limits of the ratio range are shown at the bottom of the panels. (D) Average of FRET/TFP ratio of Matrigel-contacting (bottom) and -non-contacting (top) areas in each FRET image of Fig. S4C was calculated to obtain FRET efficiency (Raichu-Rac1 : siWnt5a, n=15, siDvls, n=15; Raichu-RhoA : siWnt5a, n=11, siDvls, n=12). The relative FRET efficiency in Matrigel-contacting area (bottom) was expressed compared with that in non-contacting area (top). (E) IEC6 cells stably expressing Raichu-Rac1 or Raichu-RhoA were plated on type I collagen gel in a glass-bottomed dish for 2 h. Representative FRET/TFP ratio images in type I collagen-contacting area (bottom) and -non-contacting area (top) are shown in the intensity-modulated display mode. The upper and lower limits of the ratio range are shown at the bottom of the panels. (F) Average of FRET/TFP ratio of type I collagen-contacting (bottom) or -non-contacting (top) areas in each FRET image of Fig. S4E was calculated to obtain FRET efficiency (Raichu-Rac1, n=9; Raichu-RhoA, n=9). The relative FRET efficiency in type I collagen-contacting area (bottom) was expressed compared with that in non-contacting area (top). The results are shown as means ± SD from three independent experiments. $*P<0.01$. Scale bars in (C) and (E), 5 μm.

Supplemental Figure S5. Wnt5a, Dvl and Tiam1 were involved in Rac1 activation induced by adhesion to Matrigel. (A) Wnt5a- or Dvls-depleted IEC6 cells cultured on Matrigel for 1 h were lysed and subjected to the Rac1 assay. Fold changes of Rac1 activity are shown as means from three independent experiments. (B) GFP-, GFP-Dvl2-, or Myc-Tiam1-expressing IEC6 cells were transfected with the indicated siRNAs and the cells were plated on Matrigel for 1 h. The lysates were subjected to the Rac1 assay. (C) Tiam1-depleted Raichu-Rac1 expressing IEC6 cells were plated on Matrigel in a glass-bottomed dish for 2 h. Representative FRET/TFP ratio images in Matrigel-contacting area (bottom) and -non-contacting area (top) are shown in the intensity-modulated display mode. The upper and lower limits of the ratio range are

shown at the bottom of the panels. (D) Average of FRET/TFP ratio of Matrigel-contacting (bottom) or -non-contacting (top) area in each FRET image of Fig. S5C was calculated to obtain FRET efficiency (n=14). The relative FRET efficiency in Matrigel-contacting area (bottom) was expressed compared with that in non-contacting area (top). The results are shown as means ± SD from three independent experiments. **P*<0.01. Scale bar in (C), 5 μm.

Supplemental Figure S6. Wnt5a signaling regulates RhoA activity through FAK and p190RhoGAP-A and the polarized localization of p190RhoGAP-A. (A) Wnt5a- or Dvls-depleted IEC6 cells cultured on Matrigel for 2 h were lysed and probed with the indicated antibodies. (B) IEC6 cells treated with PF573228 were plated on Matrigel for 2 h. The numbers of polarized cells among total cells were counted, and the percentages of polarized cells were calculated. The ratios of the percentages of polarized cells were compared with the controls. The results are shown as means ± SD from three independent experiments. **P*<0.01. (C) PF573228-treated IEC6 cells cultured on Matrigel for 1 h were lysed and subjected to RhoA and Rac1 assays. Fold changes of RhoA and Rac1 activities are shown as means from three independent experiments. (D) Wnt5a- or Dvls-depleted GFP-p190RhoGAP-A expressing IEC6 cells cultured on Matrigel for 2 h were stained for GFP (green) and F-actin (red). Scale bar, 5 μm.

Supplemental Figure S7. Dvl binds to Tiam1 and p190RhoGAP-A. (A) (Upper panels) GFP-Dvl2-deletion mutants were expressed in HEK293T cells stably expressing p190RhoGAP-A and the lysates were immunoprecipitated with anti-p190RhoGAP-A antibody. The immunoprecipitates were probed with anti-GFP and anti-p190RhoGAP-A antibodies. Arrowheads indicate GFP-Dvl2 (WT), ΔDEP and GFP-Dvl2 (506-736) coimmunoprecipitated with p190RhoGAP-A. (Lower panel) Regions of Dvl2 required for the interaction with p190RhoGAP-A are shown. Amino acid numbers are indicated. (B, C, D) HA-Dvl1 deletion mutants were expressed in HEK293T cells stably expressing GFP-p190RhoGAP-A (B and D, right panels) or Myc-Tiam1 (C and D, left panels) and the lysates were immunoprecipitated with anti-GFP or anti-Myc antibody. The immunoprecipitates were probed with anti-HA and anti-GFP or anti-Myc antibodies. Arrowheads indicate HA-Dvl1 deletion mutants coimmunoprecipitated with GFP-p190RhoGAP-A or Myc-Tiam1. Regions of Dvl1 required for the interaction with GFP-p190RhoGAP-A or Myc-Tiam1 are shown in (B) (lower panel). Amino acid numbers are indicated.

Supplemental Figure S8. The formation of basolateral membrane in IEC6 cysts treated with NSC23766, Y27632, or PF573228. IEC6 cells treated with NSC23766, Y27632, or PF573228 were plated on Matrigel for 72 h and stained for pEzrin (green), β-catenin (red), and DRAQ5 (blue). The lower panel of each cyst shows an enlarged image of the area within the dashed boxes. Right panels indicate the relative intensity of β-catenin staining from outer to apical membrane (along the arrow). Scale bar, 10 μm.

Supplemental Figure S9. A proposed model for adhesion-dependent single-cell polarization. See discussion.

Supplemental Figure S1

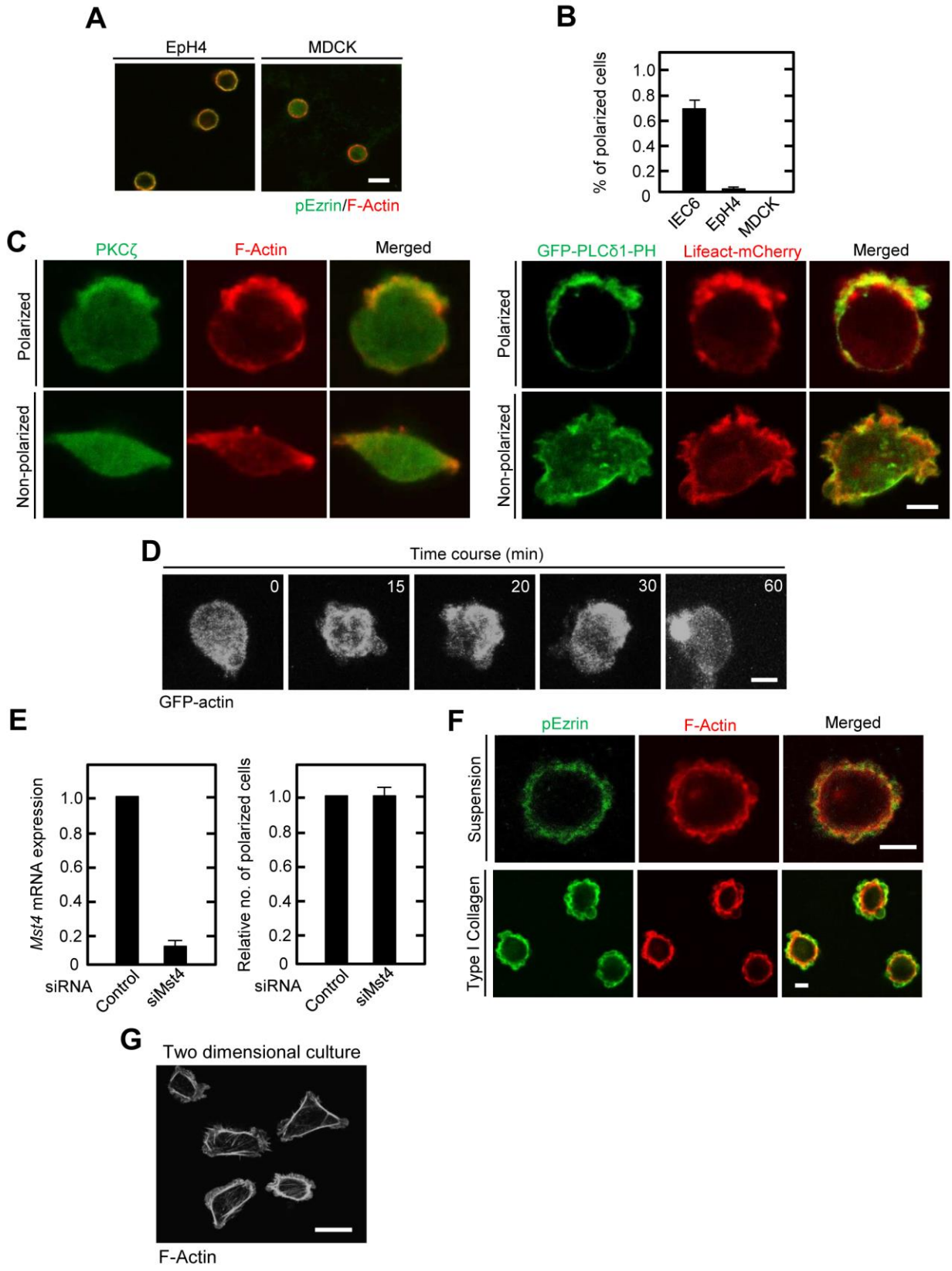

Supplemental Figure S2

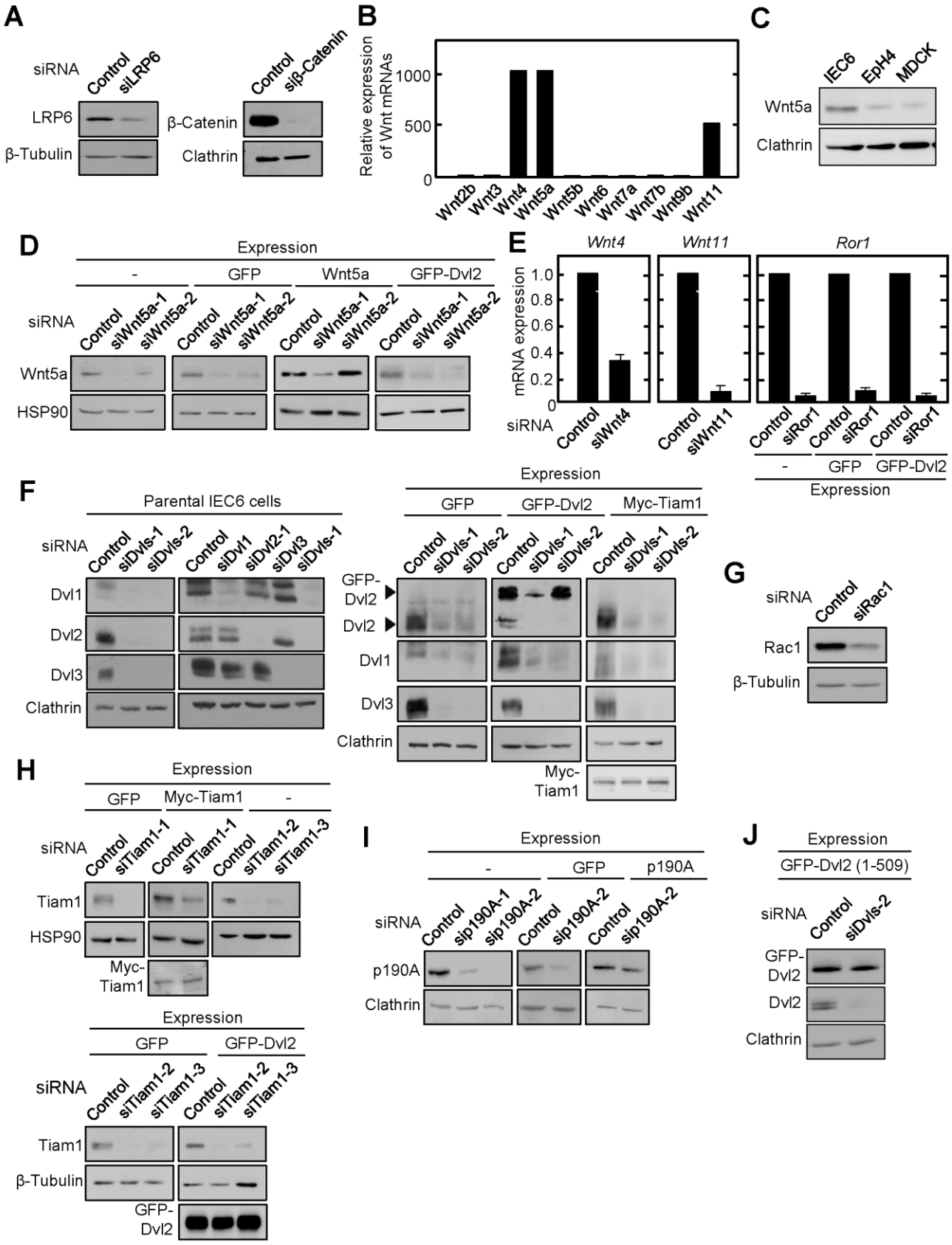

Supplemental Figure S3

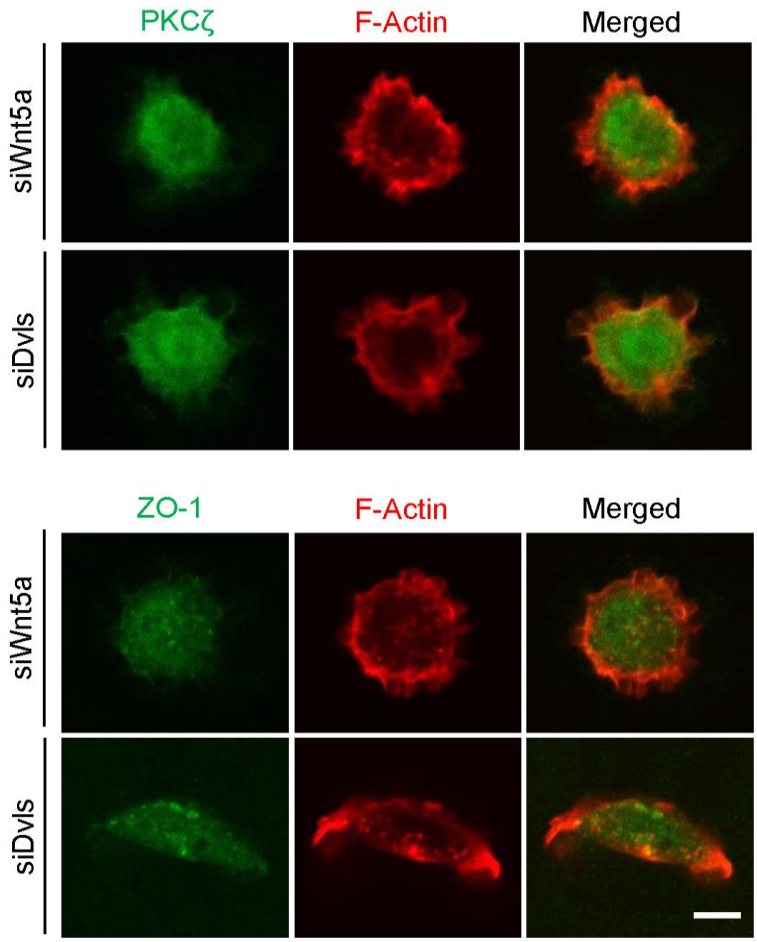

Supplemental Figure S4

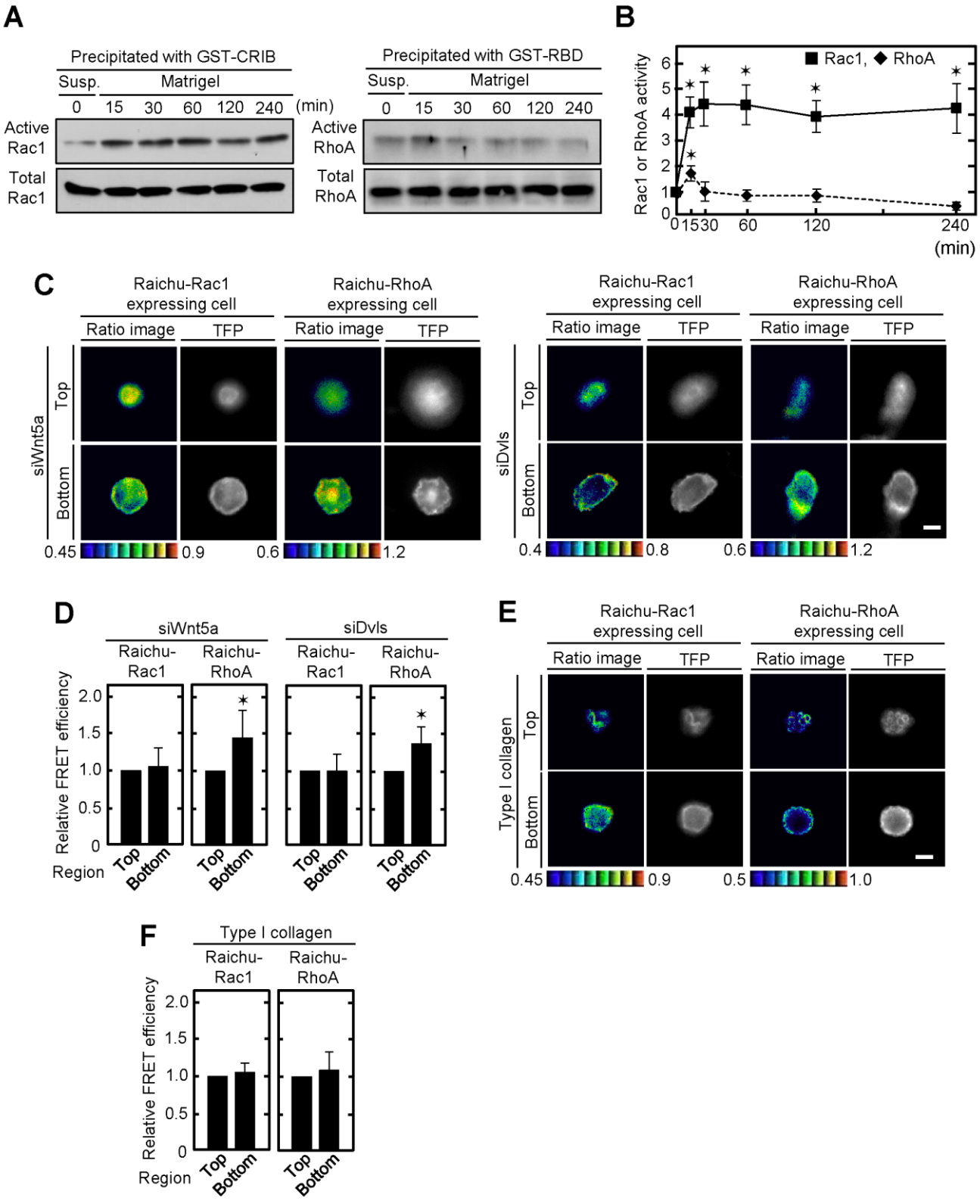

Supplemental Figure S5

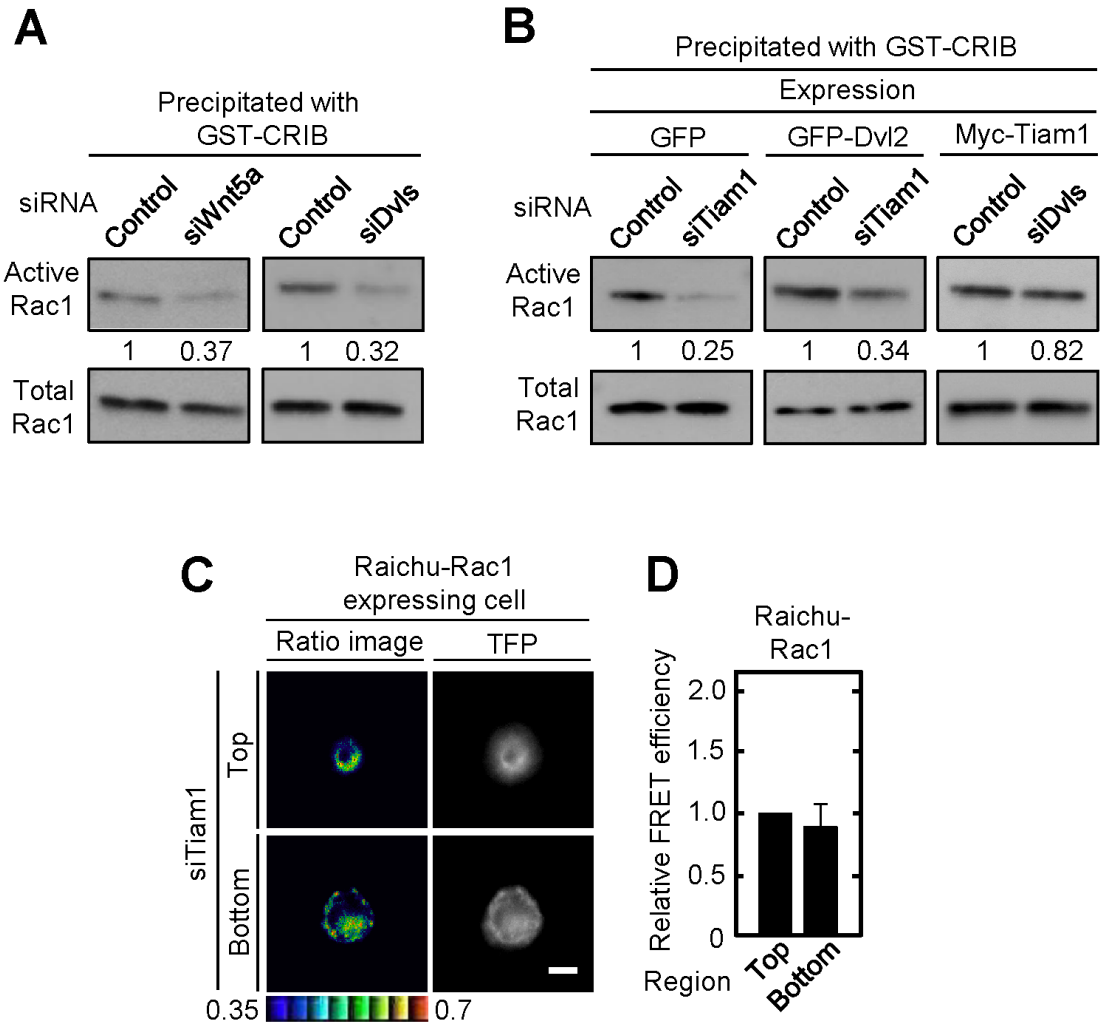

Supplemental Figure S6

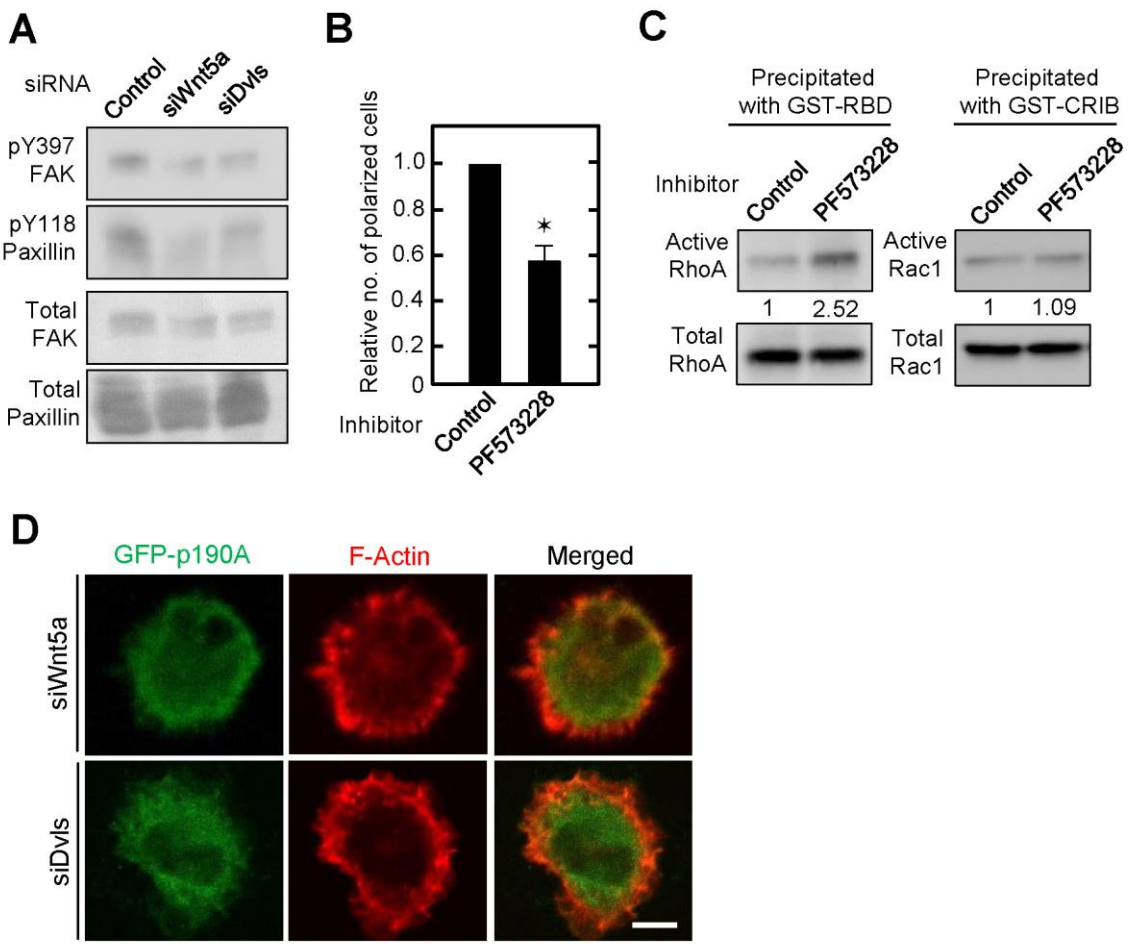

Supplemental Figure S7

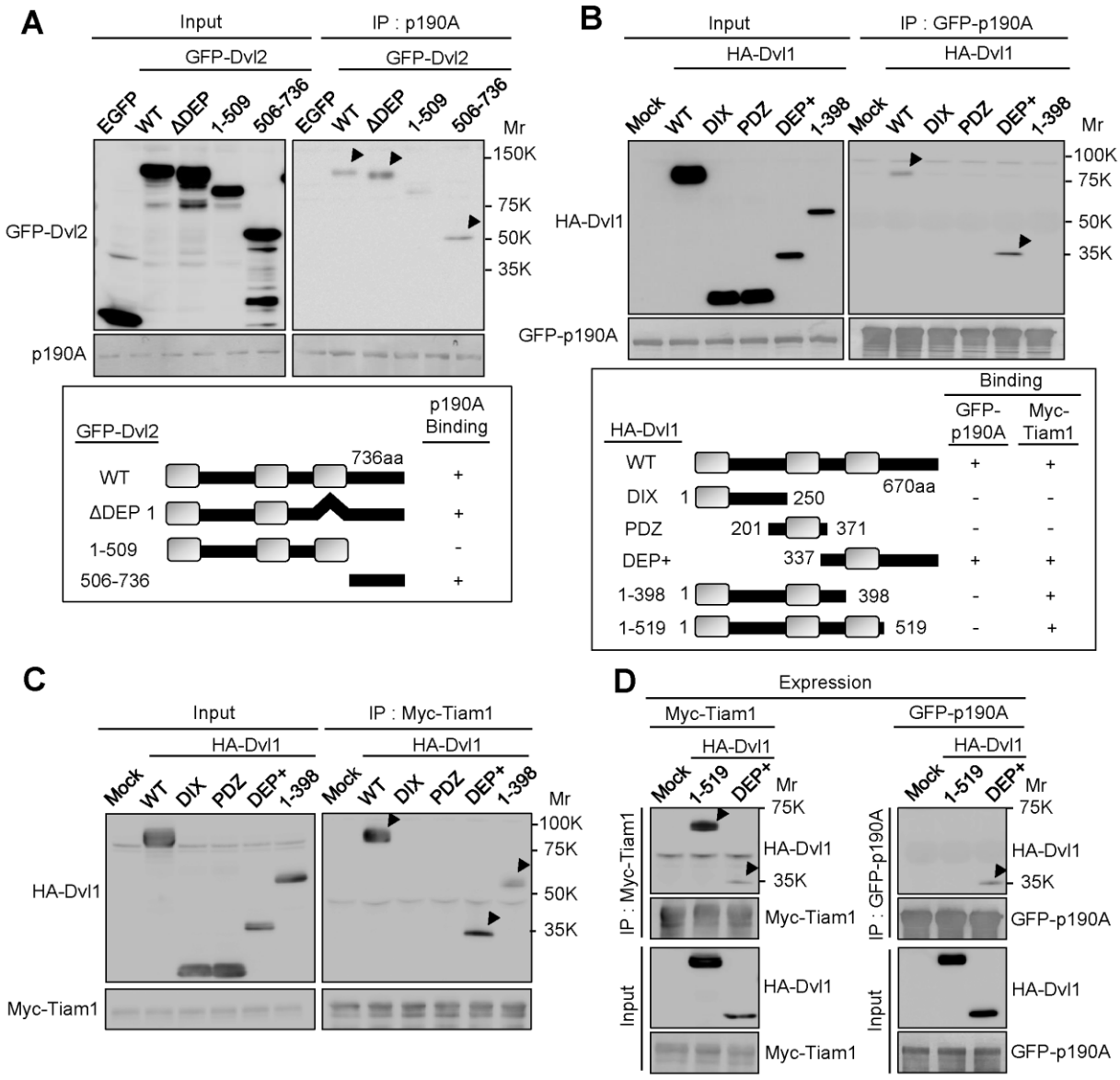

Supplemental Figure S8

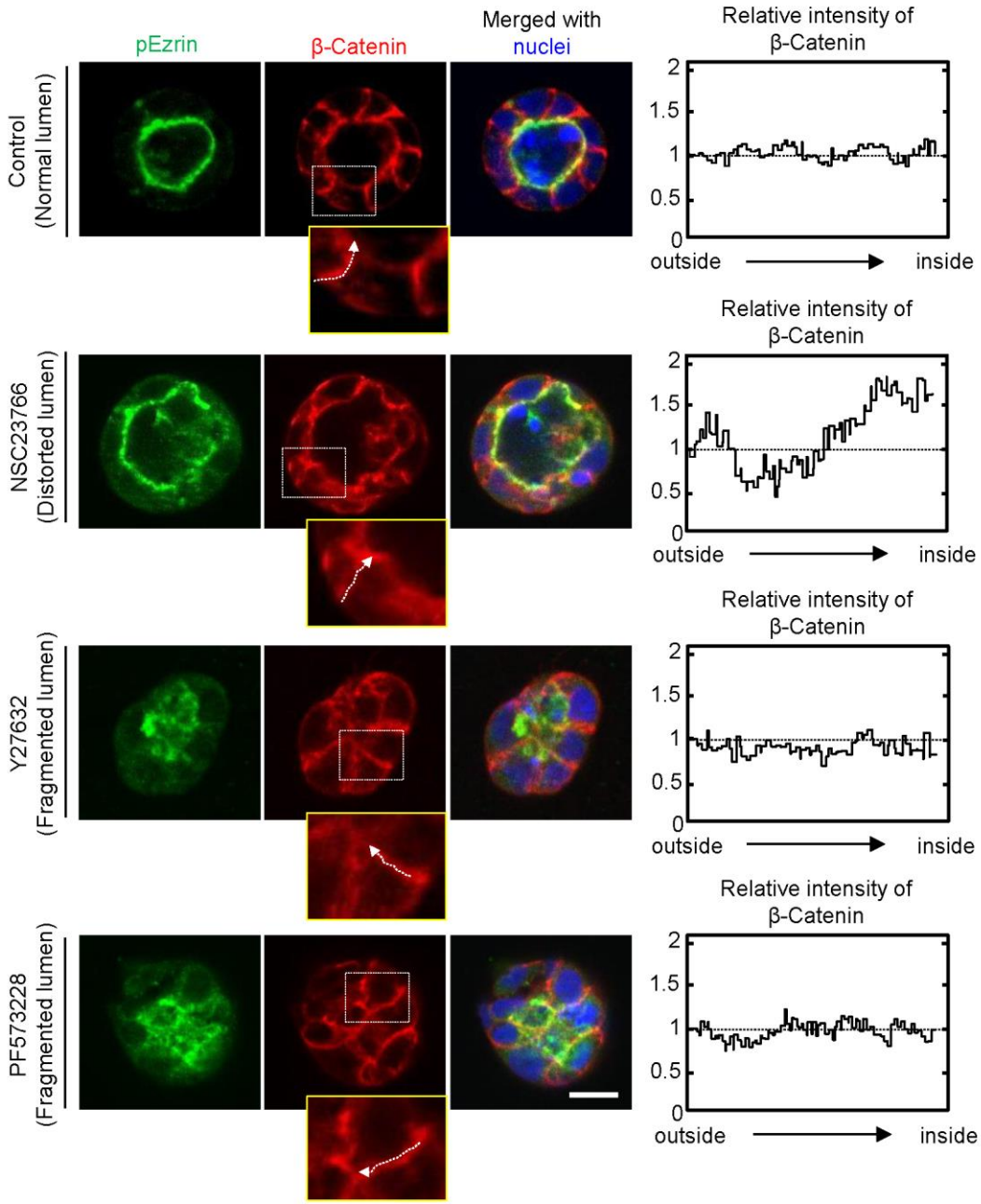

Supplemental Figure S9

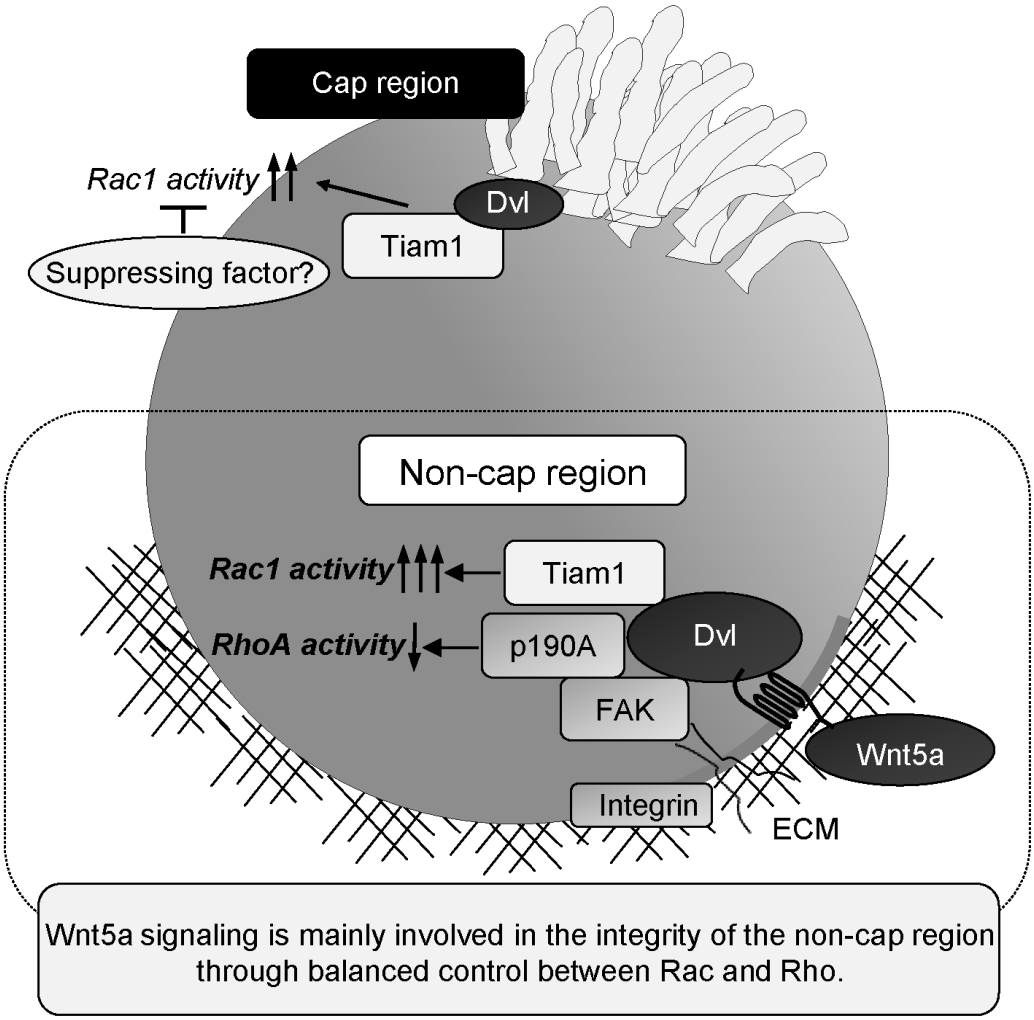

Wnt5a signaling is mainly involved in the integrity of the non-cap region through balanced control between Rac and Rho.

Company	Name	Used for
Abcam	Rabbit anti-Ezrin (phospho T567)	IF
	Rabbit anti-Tiam1	IB
Aves Labs	Chicken anti-GFP	IF
BD Biosciences	Mouse anti-β-catenin	IB, IF
	Mouse anti-Clathrin	IB
	Mouse anti-HSP90	IB
	Mouse anti-Rac1	IB
	Mouse anti-FAK	IB
	Mouse anti-Paxillin	IB
Cell Signaling Technology	Rabbit anti-Wnt5a/b	IB
	Rabbit anti-LRP-6	IB
	Rabbit anti-Dvl2	IB, IF
	Rabbit anti-Dvl3	IB
	Rabbit anti-RhoA	IB
	Rabbit anti-p190RhoGAP-A	IB, IP
	Rabbit anti-Paxillin pY118	IB
Invitrogen	Rabbit anti-ZO-1	IF
	Rabbit anti-FAK pY397	IB
	Rabbit anti-GFP	IF, IP
Medical & Biological Laboratories	Rabbit anti-HA	IB
	Rabbit anti-Myc	IB
Millipore	Mouse anti-phosphotyrosine	IB
Santa Cruz Biotechnology	Rabbit anti-PKCζ	IF
	Mouse anti-GFP	IB
Sigma-Aldrich	Mouse anti-β-tubulin	IB
Wako	Mouse anti-FLAG	IB
	Mouse anti-HA	IB

Table S1. The antibodies used in this study.

Name	Base sequence
Randomized control	5’-CAGTCGCGTTTGCGACTGG-3’
rat Wnt5a-1	5’-GCAAGCTGGTACAGGTCAA-3’
rat Wnt5a-2	5’-CCAGGACCCACATATTTAT-3’
rat Ror1	5’-GGCATTGCATGTGCACGAT-3’
rat Dvl1	5’-CCAGTAGCCGAGATGGAAT-3’
rat Dvl2-1	5’-GCGAGACGAAGGTGATTTA-3’
rat Dvl2-2	5’-GCCCTTGGCCTGGTAAGTT-3’
rat Dvl3	5’-GCATCACAGACTCCACTAT-3’
rat Wnt4	5’-GCGCAGTTCAAGCCACATA-3’
rat Wnt11	5’-GCATCAAAGGAAACTGATA-3’
rat LRP6	5’-GCAGCCAAATGCTACAAAT-3’
rat β-catenin	5’-CCATGGAGCCAGACAGAAA-3’
rat Rac1	5’-GCAAACAGACGTGTTCTTA-3’
rat Tiam1-1	5’-CCTCTTAGGTCGCACTCTT-3’
rat Tiam1-2	5’-GCGCACCAACTGGATCATT-3’
rat Tiam1-3	5’-CCAATAATCAGCCAGCCTT-3’
rat p190RhoGAP-A-1	5’-GCCTCAGGATGGATTTGAT-3’
rat p190RhoGAP-A-2	5’-GCAAGGTACAAATGTGTTA-3’
rat Mst4	5’-GGGTCCTATCTAAAGGGTT-3’

Table S2. The RNA duplexes used in this study.

Name	Base sequence of forward and reverse primers
rat GAPDH	5’-ATCAACGACCCCTTCA-3’ and 5’-TTTGGCCCCACCCTTC-3’
rat Wnt2b	5’-ACTGGGGTGGCTGTAGTGAC-3’ and 5’-GTACGGCGGAAGTCTGAGAG-3’
rat Wnt3	5’-TGTGAGGTGAAGACCTGCTG-3’ and 5’-AAAGTTGGGGGAGTTCTCGT-3’
rat Wnt4	5’-GCCACGCACTAAAGGAGAAG-3’ and 5’-GGCCTTAGACGTCTTGTTGC-3’
rat Wnt5a	5’-AAGACGGGCATCAAAGAGTG-3’ and 5’-TGCAACCACAGGTAGACAGC-3’
rat Wnt5b	5’-TGACTACTGCCTGCGAAATG-3’ and 5’-AAAGCAACACCAGTGGAACC-3’
rat Wnt6	5’-GTCGACTTTGGGGATGAGAA-3’ and 5’-AAAGCCCATGGCACTTACAC-3’
rat Wnt7a	5’-AGGACTGGGAGCTGAGAACA-3’ and 5’-GCAGCAAACAGCAAAAACAA-3’
rat Wnt7b	5’-GCTATCAGAAGCCGATGGAG-3’ and 5’-ACGTGTTGCACTTGACGAAG-3’
rat Wnt9b	5’-CTGGAGTGTGCCCTACCAAT-3’ and 5’-CAGGCTTGGCAAGGACTTAG-3’
rat Wnt11	5’-CAGGATCCCAAGCCAATAAA-3’ and 5’-TAGGCCGGTGTACCACTTTC-3’
rat Mst4	5’-TTTTGAGTCAGTGCGACAGC-3’ and 5’-TGGCAATCTGGAATTCATCA-3’
rat Ror1	5’-CAAGAAAGTGGTTTCTACCA-3’ and 5’-ACTTCACATTCATCCCGACA-3’

Table S3. Forward and reverse qPCR primers used in this study.